

# Ground Calibration of an Orbiting Spacecraft Transmitter

Jon T. Adams  
Jet Propulsion Laboratory  
4800 Oak Grove Drive  
Pasadena, CA 91109  
818-354-3445  
[jta@jpl.nasa.gov](mailto:jta@jpl.nasa.gov)

James P. Lux  
Jet Propulsion Laboratory  
4800 Oak Grove Drive  
Pasadena, CA 91109  
818-354-2075  
[jimlux@jpl.nasa.gov](mailto:jimlux@jpl.nasa.gov)

*Abstract*— The SeaWinds Calibration Ground Station (CGS) is a novel Ku-band receiving station that supports the June 1999-launched JPL/NASA SeaWinds scatterometer radar which measures the near-surface wind speeds over 90% of the ice-free oceans. The CGS purpose is to measure very accurately the radar pulse timing, frequency and amplitude characteristics in order to monitor independently the radar and spacecraft platform performance over the course of the mission. These data are critical to maintaining or improving the quality of the end-data product. Results are presented here which show the ability to measure spacecraft pulse timing to microsecond detail, spacecraft attitude to better than 0.1 degrees, and output amplitude that will in future work allow estimation of the spacecraft on-orbit antenna pattern. These efforts will improve registration of the scatterometer-derived wind map to the Earth's coordinate system and provide an independent assessment of the instrument quality over the life of the mission.

direction. Analysis of the  $\sigma^0$  data allows the derivation of an estimate of the wind velocity vector for that patch.

The SeaWinds instrument has an 803 km circular orbit and uses a rotating, 0.85 meter offset paraboloid antenna to produce a pair of conically scanned pencil beams at nominal angles of 40 and 46 degrees from the nadir. The beams illuminate an elliptical footprint on the sea surface of about 25 km wide by 50 km deep (major axis is radial from the spacecraft nadir-point). On board processing of the echo data allows resolution improvement to slices 25km wide by about 6 km deep. Spacecraft platform attitude instabilities can greatly affect the ability to accurately register the reduced wind vector map with the actual position on the earth; unobserved instrument frequency and Doppler estimation variation provide a mechanism to force incorrect range measurement, again affecting eventual data registration; and instrument amplitude and gain variation can cause errors in the estimation of received echo strength and thus the derived wind velocity vector. All of these effects were observed to some extent on a predecessor instrument, NSCAT, which was in a similar orbit during 1996-97. There are a variety of methods that can provide partial calibration, including natural ground targets such as the Antarctic and Greenland ice sheets and the Brazilian rain forest, in addition to the detailed telemetry from the spacecraft itself.

## TABLE OF CONTENTS

1. INTRODUCTION
2. CGS DESIGN
3. CALIBRATION
4. DATA PROCESSING AND DISTRIBUTION
5. SAMPLE SPACECRAFT SIGNAL MEASUREMENTS
6. CONCLUSIONS

### 1. INTRODUCTION

The SeaWinds Calibration Ground Station (CGS) is a novel Ku-band receiving station that supports the JPL/NASA SeaWinds scatterometer radar which measures the near-surface wind speeds over 90% of the ice-free oceans. The SeaWinds scatterometer is a Ku-band (13,402 MHz) radar that obliquely illuminates the ocean's surface with the radar beam and measures the scattering cross section,  $\sigma^0$ , from a plurality of azimuth angles. For a given patch of sea surface, The  $\sigma^0$  varies in an approximately cosinusoidal manner depending on illumination azimuth angle, surface wind speed and

The Jet Propulsion Laboratory (JPL) SeaWinds Calibration Ground Station (CGS), located at the NASA-Johnson Space Center White Sands Test Facility at Las Cruces, New Mexico, is not only a precision receiver and an accurate time and frequency measurement device but also a radiometer that provides the ability to calibrate the receiver by using both sky and local targets of very accurately known temperature and stability. The CGS antenna captures the incident signal, which is then digitized, decimated and streamed into a one Gigabyte buffer prior to being written to disk. Initially, the large volume of data is scanned to identify the approximate pulse timing. Then, more

extensive processing using an iterative matched filtering technique accurately locates the precise beginning and end of each received pulse, the pulse center frequency and Doppler shift, in addition to determining the total pulse power and pulse amplitude characteristics.

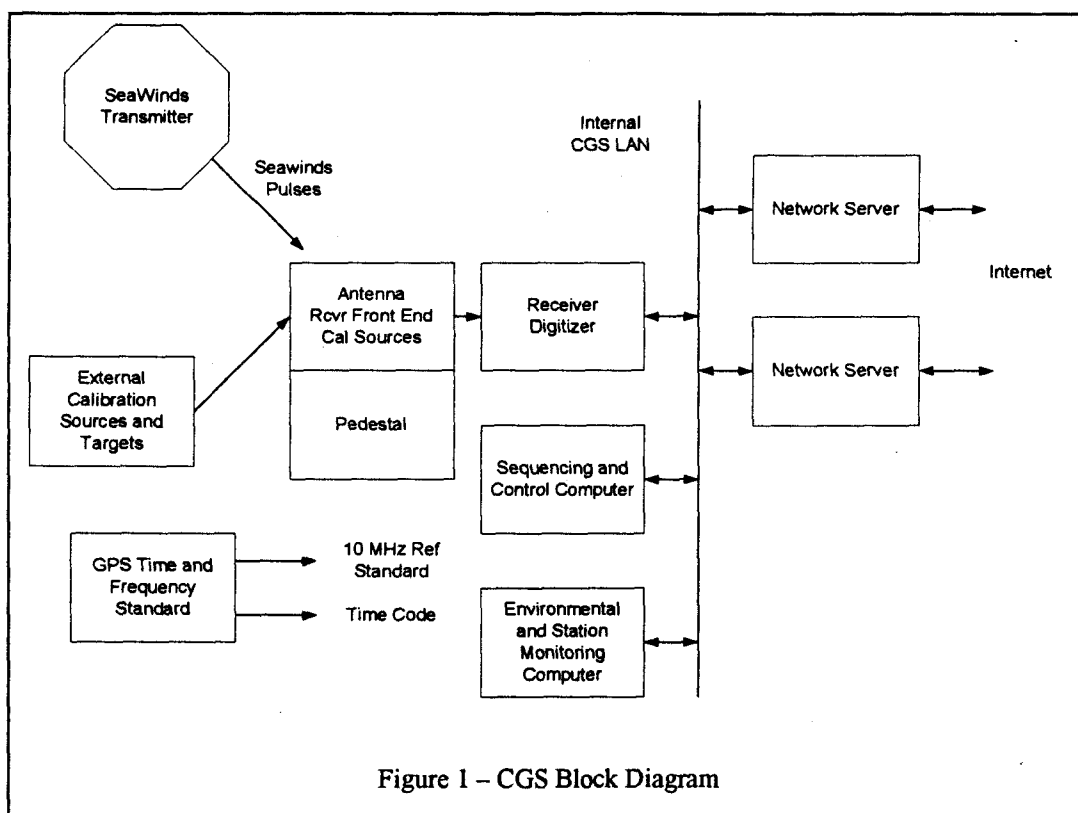
This data has so far proven extremely valuable in helping to resolve spacecraft attitude control issues, orbital variation and spacecraft on-board clock anomalies. Future work is planned to use the amplitude and timing data to help reconstruct the actual on-orbit spacecraft antenna pattern, especially with respect to sidelobe shape and level.

## 2. CGS DESIGN

The core of the CGS is a fairly straightforward dual conversion super-heterodyne receiver with the final signal processing done in the digital domain. The receiver is packaged to increase thermal stability. Internal and external reference sources are provided to allow self calibration.

A computer controlled pedestal is used to point the CGS antenna at the predicted spacecraft location. The receiver front end, as well as the calibration sources, are located in an insulated steel and aluminum box on the pedestal, within a fiberglass and Nomex® composite radome on top of the building.

A pair of independent data communications links allow access to the CGS servers via the internet in



### Overview

The CGS is installed in a temperature controlled building at White Sands Test Facility near Las Cruces, New Mexico. Figure 1 shows a block diagram of the CGS, which consists of a high performance receiver, a number of PC type computers, calibration standards and sources, a GPS time and frequency standard, and environmental monitoring equipment.

a redundant fashion. Once a day, data from the CGS is mirrored to a server at the Jet Propulsion Laboratory Physical Oceanography Distributed Active Archive Center (PODAAC). CGS data users can retrieve the data from either the CGS directly, or from PO.DAAC.

### Antenna and Radome

The antenna is a conical corrugated horn with an aperture of 12 cm designed to have a maximum gain variation of 0.01 dB within 1 degree of boresight. This reduces the pointing accuracy

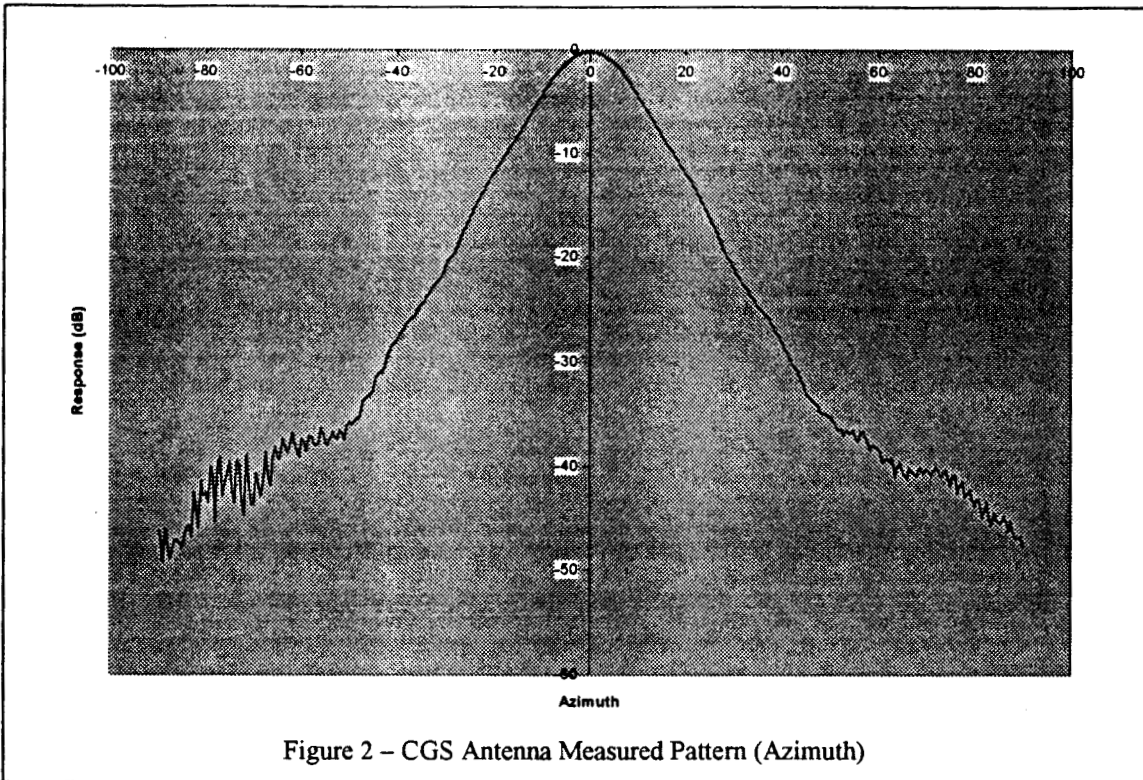


Figure 2 – CGS Antenna Measured Pattern (Azimuth)

requirements, which are influenced by both the predicted ephemeris accuracy and the pedestal pointing accuracy. Figure 2 shows the measured antenna pattern in the azimuth axis.

The SeaWinds signals are linearly polarized (inner beam horizontal, outer beam vertical). A circularly

polarized antenna reduces the effect of the absolute rotational orientation of the antenna, and eliminates the need to switch between antennas to receive the different signals. A circular to linear transformation section between the circular horn throat and the rectangular WR-62 waveguide to the receiver is used to make the antenna subsystem circularly

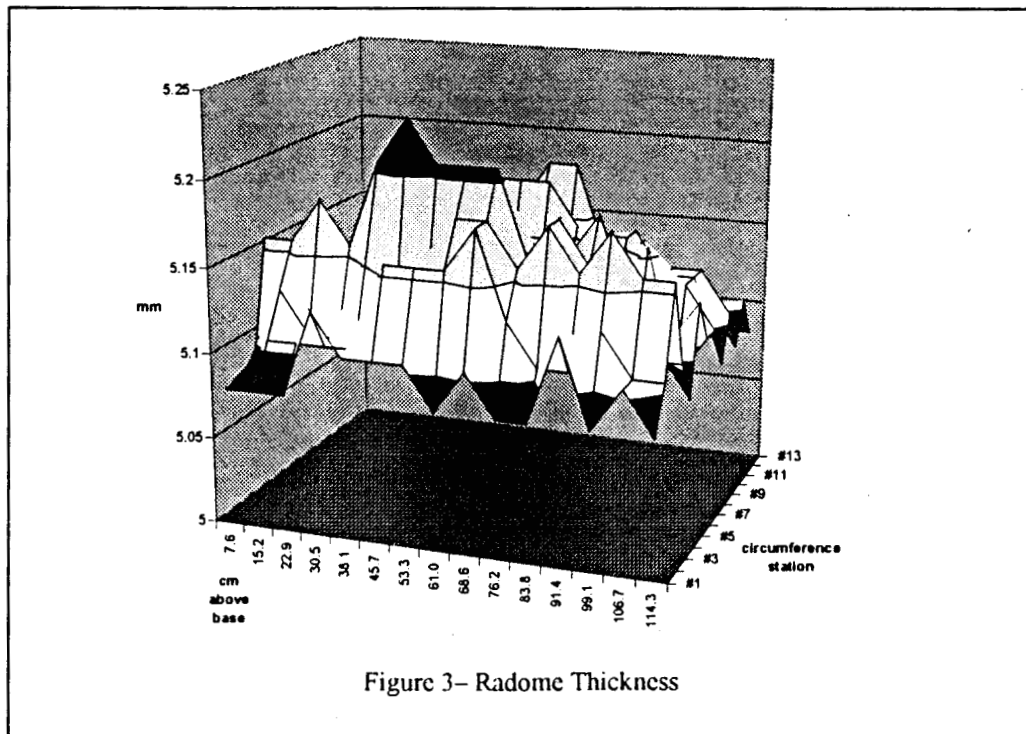


Figure 3– Radome Thickness

polarized with the entire subsystem having an axial ratio of <math><0.5\text{ dB}</math>. A 2 degree error in rotational position (axis along the boresight) will result in a system gain error of less than 0.01 dB.

The directivity of the antenna, as calculated from integrated pattern measurements, is 20.09 dB, which compares well with the design directivity of 20 dB. Note that because of the circular polarization, the received signal, which is linearly polarized, will be attenuated by 3 dB.

The receiver front end (and antenna) is mounted on an elevation over azimuth pedestal within a fiberglass and Nomex® honeycomb composite radome on top of the CGS building. The radome is a 1.2 meter diameter cylinder with 1.5 meter tall vertical sides, which reduces the chances of dew or dust collecting on the surface. The central axis matches that of the pedestal, so that the incidence angle or distance from the aperture to the radome wall does not change with azimuth at a particular elevation angle. The mechanical dimensions of the radome were carefully controlled to minimize changes in attenuation with look angle. The measured variations in the 5.08 mm thick composite wall (shown in Figure 3), are on the order of .033 mm, and are calculated to result in loss variations of less than 0.01 dB. Actual radome

loss is being measured using a radiometric technique described by Seidel and Stelzreid<sup>2</sup>, involving scanning the cold night sky (and the radome) using the CGS receiver as a radiometer.

#### Receiver Electronics

The receiver (block diagram in Figure 4) is a standard double conversion superheterodyne with a first IF of 395 MHz and an output frequency of 35 MHz. The final conversion to baseband is done by undersampling at a final rate of 5.1875 MSPS, which effectively places the signal at  $\frac{3}{4}$  of the sample rate. The mechanical packaging was designed to keep the temperatures stable during a measurement, to reduce gain fluctuations. Internal calibration sources are provided to calibrate the receiver gain. Frequency and timing accuracy are determined by the design, and require no calibration.

The receiver is physically divided into two parts. The first part, referred to as the "antenna box" is a steel enclosure approximately 76x60 cm mounted on a 1 cm aluminum plate which is on the pedestal in the radome. The entire enclosure is covered in radar absorber to reduce the effect of reflections affecting the antenna pattern, and to provide some thermal isolation from the environment. There are also three precision resistance thermometers (4

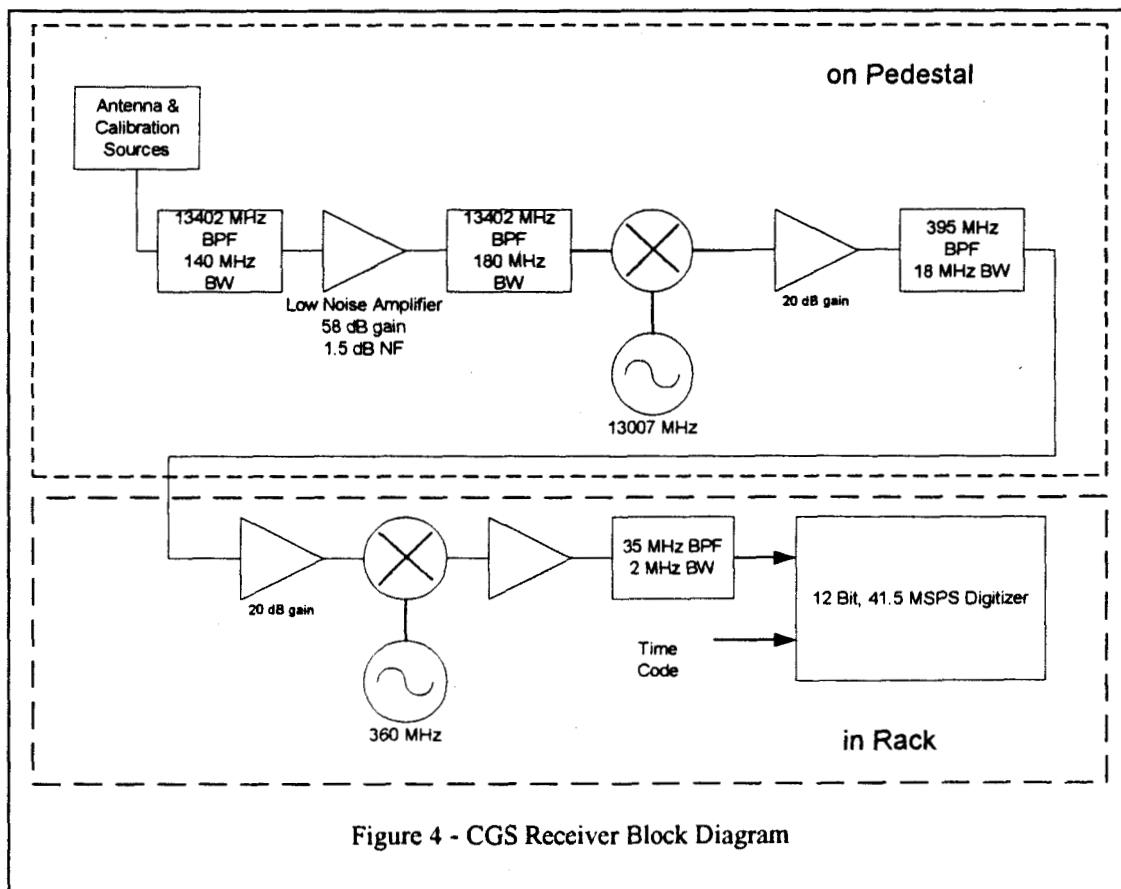


Figure 4 - CGS Receiver Block Diagram

wire RTDs) inside the enclosure which are used to log the receiver temperature. The second half of the receiver is in a standard chassis in the equipment rack located below the pedestal in the air-conditioned room.

A low noise amplifier at 13402 MHz is used to set the system noise figure as well as provide some 50 dB of gain before the first mixer. A local oscillator at 13007 MHz (phase locked to the 10 MHz reference) is used to mix to a 395 MHz first IF. This IF signal is carried by coaxial cable to the receiver chassis.

In the receiver chassis, the 395 MHz IF is mixed with a 360 MHz local oscillator (also locked to the 10 MHz reference) to produce an output signal at 35 MHz nominal center frequency. A 2 MHz bandwidth Butterworth filter is used to limit the bandwidth prior to sampling.

The data is sampled by a commercial high speed 12 bit A/D board (Gage PCI-8012A) modified to accept a 41.5 MHz external clock derived from the stable 10 MHz reference. The board internally decimates the samples by a factor of 8, resulting in an actual sample rate of 5.1875 Megasamples/Second. The 35 MHz IF is aliased to an apparent frequency of -1.3125 MHz, which is approximately in the middle of the sampled bandwidth of approximately 2.6 MHz, which keeps the desired signal away from DC offsets and sample clock related spurs. The system gain is set so that the maximum received signals are about 3dB below A/D saturation. The total digitized noise power (looking at a cloudy sky) has a standard deviation of 13.4 LSB, or about -44 dBFS.

In a typical capture, 10 seconds of data is collected for each of 4 beam crossings, as the two spacecraft-transmitted beams sweep over the CGS. On days when only the outer beam crosses the CGS, two captures of 20 seconds each are made. The 1 Gbyte memory buffer available allows collection of up to 51 seconds of data, when recording the IRIG time code on the second channel.

Absolute frequency stability is maintained by the use of a GPS disciplined 10 MHz reference oscillator, which is used to generate all local oscillators and the sampling clock. The oscillator is specified to be accurate within 1 part in 1E12 over 1 day. IRIG-B time code from the GPS receiver is digitized simultaneously to provide an independent check on the capture timing. In addition, the 1 PPS output from the GPS receiver is used to synchronize the start of data captures, so that absolute sample time is known to approximately 200 nSec. The GPS receiver also provides an accurate position (averaged over time) of the CGS, which is necessary to calculate ranges and actual look angles in post processing.

#### Computers and support equipment

The CGS is controlled by a set of 5 PC type computers running Windows NT®. They are interconnected by a 100 Mbps ethernet. One PC is dedicated to the high speed data acquisition interface. Another is used to control the pedestal, operate the calibration equipment, and log various engineering parameters. A third is used to capture video images and provide other support functions. Finally, two computers are servers which connect to separate redundant connections to the internet; one via WSTF's internal network and the other via a microwave link to White Sands Missile Range.

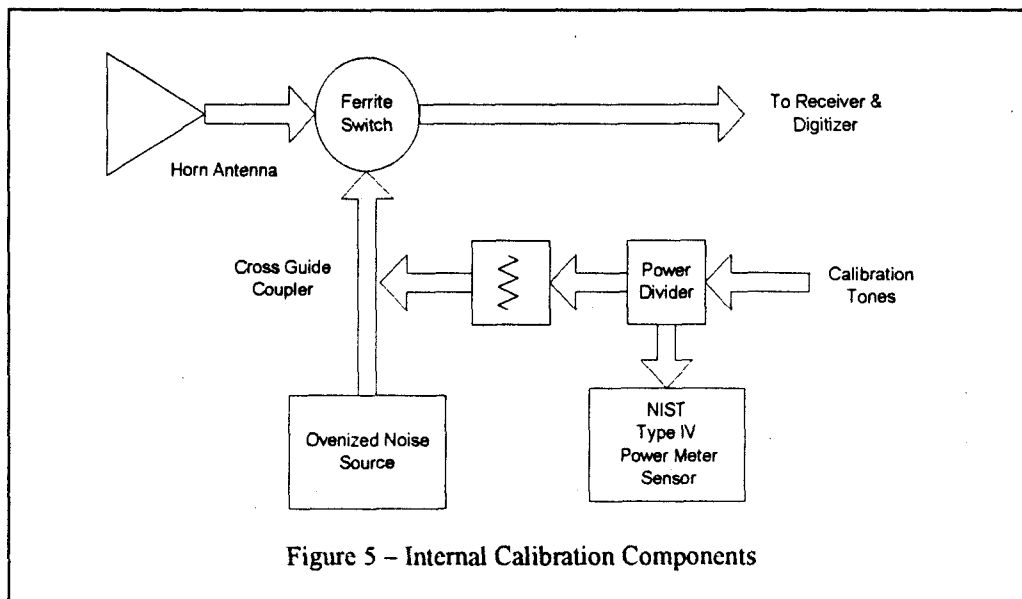


Figure 5 - Internal Calibration Components

### 3. CALIBRATION

Calibration of the CGS is accomplished by using both external references and internal sources. Internal precision sources provide a stable gain calibration. A remote controlled beacon transmitter on a hill top about 3 km away provides an end to end functional test as well as a test of antenna pattern. Figure 5 illustrates the calibration equipment within the pedestal mounted enclosure (the "antenna box").

#### *Self Calibration*

The CGS provides several ways of being self calibrated against an internal stable reference. A single ferrite switch is used to connect the LNA input to a calibration source instead of the antenna. To reduce the effect of mismatch on the antenna port, during calibrations, the antenna is pointed at either cold sky or at an RF absorber panel mounted on the inside of the radome.

The calibration path consists of a switched noise source and a tone injection path. The noise source has an ENR of 14.491 dB, and so, provides a test signal near the bottom of the system dynamic range (The kTB noise floor is -111 dBm). There is also provision for injecting an externally supplied tone at a level of about -75 dBm, which corresponds to the top of the dynamic range.

The noise source is the most accurate level reference. It is based on a semiconductor noise diode which has a noise brightness temperature of 8446K ( $2\sigma$  uncertainty = 53K), or an ENR of 14.491 dB. The noise source is placed in an insulated enclosure which is thermostatically controlled to 40 degrees Celsius within .05 degrees. This "oven" is located within the thermally massive and insulated receiver box on the pedestal. Stability measurements performed at NIST using their WR-62 radiometer indicate that the noise power output of the noise source does not vary over a 4 day period by more than the uncertainty of the radiometer (about 10 K). The output power of the receiver is measured by calculating the variance of the digitized samples.

In addition, a tone signal may be injected through a calibrated path at the same point as the noise signal. The power of the injected signal is measured by a NIST Type IV Power meter<sup>5</sup> at approximately 0 dBm prior to being attenuated approximately 70 dB. The calibration tone is generated by a standard laboratory synthesized signal generator (HP model 8673C). Tone signals are useful for evaluating the performance of the

digitizer, with the usual analysis technique consisting of fitting a sine wave to the digitized samples, and examining the deviations from the ideal.

For highest accuracy, self calibrations cannot be done while the spacecraft is above the horizon. The sidelobes of the SeaWinds antenna are 30-40 dB below the main lobe, which is approximately at the thermal noise floor of the receiver, and are easily detected with a radiometric approach.

#### *Daily Radiometric Gain Calibrations*

Each morning, at 1115Z (approximately 415AM local), a radiometric gain calibration is performed, making 0.2 second measurements of the ovenized noise source, the ovenized load, and the sky. This schedule was established prior to launch, and a potential problems has been identified because the spacecraft is above the horizon at this time on "day 1" of the cycle during the revolution (100 minutes) before the "morning" capture. A change in the scheduled radiometric calibration time to an earlier time is planned to eliminate the possibility of the measurement being corrupted by sidelobe power. Figure 6 shows the results of this calibration over a several month time span.

The raw gain is calculated by comparing the variances of the sampled data when the noise source is on ( $T=8446K$ ) and off ( $T=313K$ ). A nominal noise bandwidth of 2 MHz was assumed for this calculation, and the noise power was calculated using the nominal A/D subsystem gain to convert A/D codes to power at the A/D input.

$$Gain = \frac{\sigma_{Hot}^2 - \sigma_{Cold}^2}{kB(T_{Hot} - T_{Cold})} \quad (1)$$

where:

$$T_{Hot} = 8446K$$

$$T_{Cold} = 313K$$

There are some apparent changes in gain (on 29 July and 19 August) which are the result of the noise source oven being turned off during system maintenance activities. The overall downward trend in system gain may be an artifact, as it is less than the uncertainty in the measurement, which is at least 0.03 dB, due in large part to the 50K uncertainty in the 8446K reference.

Figure 6 also shows an estimate of the sky brightness temperature, calculated as in Eq 2:

$$T_{sky} = (\sigma_{sky}^2 - \sigma_{Cold}^2)G + T_{Cold} \quad (2)$$

where G is the gain as calculated in Equation (1).

Of particular interest in this plot are the apparent spikes in sky temperature (in mid August) which were the result of the antenna being pointed at the external ambient load (at approximately 290K) rather than the sky. The sky temperature shows

The CGS includes a weather station on the building, and logs the current wind, rainfall, temperature, humidity and barometric pressure every minute. The rain and humidity measurements can be used to evaluate whether a data capture was made when it is raining, or when there may be condensed dew or rain on the radome, either of which would reduce the accuracy of the amplitude measurements. Various other station data such as GPS receiver performance, video images of the pedestal and radome, and the receiver internal temperature is recorded periodically, and available on the CGS server.

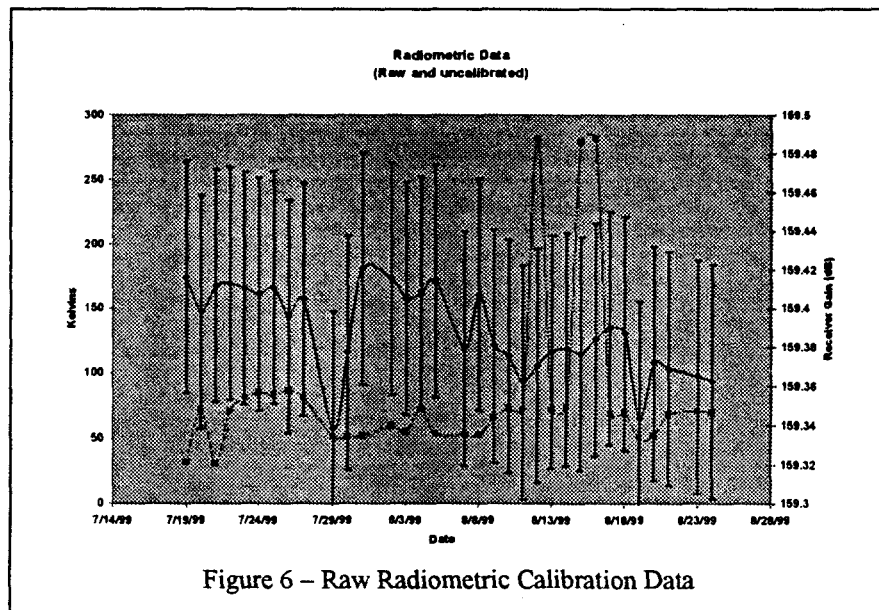


Figure 6 – Raw Radiometric Calibration Data

variations which appear to be correlated with periods of high rainfall and cloud cover. These radiometric measurements were made with the antenna pointed at the zenith, so dew, rain, or debris accumulating on the top of the radome will potentially increase the measured sky brightness temperature.

#### 4. DATA PROCESSING AND DISTRIBUTION

A significant amount of post processing is done on the raw sampled data which is collected during a spacecraft pass. Initially, the data is broken up into convenient sized files corresponding to 0.1 second of data. It is also filtered to produce a low pass filtered estimate of the received power at a lower sample rate. Approximately 14 days of raw data is maintained on the CGS, with the oldest data being removed to make room for new captures.

Two independent internet connections are used to provide redundant access to the CGS servers. The SEAPACFTP server at PO.DAAC periodically mirrors the CGS server. PO.DAAC staff makes archival backup tapes of the data, which can be used for long term studies.

#### Raw Data Reformatting

The raw captured data, originally recorded to disk as a single 1 GB block, is reformatted into files corresponding to 100 milliseconds of real time, each of which is approximately 1 Megabyte (at the 5.1875 MSPS rate). A header on the file provides the time of the capture, a text description of the capture (e.g. outer beam approaching) as well as the mean and variance of the data in the file. The variance is a convenient way to quickly find the files which have pulse data in it, since it is essentially the average received power during that time interval. The digitized IRIG time code is used to confirm the actual time of data capture.

Every few hours, catalog files listing all the raw data files and the average power estimate are created. These catalog files allow users to avoid transferring large amounts of data for time when the spacecraft antenna isn't pointing towards the CGS. Figure 7 illustrates an excerpt of this catalog file, showing the increase in average power as the edge of the outer beam crosses the station.

*Integrate and Dump Filtering*

The reformatting process also creates a filtered version of the data, which is used to find the pulses and to provide a quick means of evaluating the data. The filter is a simple integrate and dump of the squared input signal, with an *a priori* estimate of the DC bias removed. Each integrate and dump output sample is calculated as the sum of 104 input samples, providing an estimate of the received power every 20 microseconds.

$$y_k = \sum_{i=k*104}^{k*104+103} (x_i - \hat{x})^2 \quad (3)$$

At this rate (approximately 50 kSamples/Sec), the duration and timing of a single Seawinds pulse (1.5 mSec) as well as the Pulse Repetition Interval (PRI) (5.4 mSec) can be determined to within 1%.

Much higher accuracies can be achieved by utilizing multiple pulses in the calculations.

*Path loss estimate by interstitial radiometric integration*

A significant source of variability in the absolute power measurement is the atmospheric path loss. One technique to measure this is to make a radiometric measurement along the same path as the signal measurement was made and use it to calculate an estimate of the path loss (assuming nominal values for the temperature of the path) as well as the loss contribution of the radome<sup>2</sup>. Any time the spacecraft is above the horizon (about 1000 seconds) a simple radiometric measurement will include some power from the sidelobes of the spacecraft transmitter. Even very low level sidelobes can make a significant contribution to the radiometric measurement with the main lobe spacecraft signal being 30-40 dB above the noise floor.

However, the spacecraft is only transmitting during a portion (about 30%) of the pulse repetition interval. During the remaining time, in between the pulses, the received power can be integrated to develop a radiometric measurement. The integrate and dump filtered dataset provides a convenient

```

28-Oct-1999 12:05:01 CGS Raw Captured Data - Outer Approaching -
unscaled, uncalibrated - (1 of 200)

19991028120501000.raw -51.0 dBm
19991028120501100.raw -51.1 dBm
19991028120501200.raw -51.1 dBm
19991028120501300.raw -51.0 dBm
19991028120501400.raw -50.9 dBm
19991028120501500.raw -50.7 dBm
19991028120501600.raw -50.9 dBm
19991028120501700.raw -50.9 dBm
19991028120501800.raw -50.9 dBm
19991028120501900.raw -50.1 dBm
19991028120502000.raw -42.8 dBm
19991028120502100.raw -31.1 dBm
19991028120502200.raw -49.1 dBm
19991028120502300.raw -50.5 dBm
19991028120502400.raw -50.9 dBm
.
.
.

```

Figure 7 – Excerpt of CGS Raw Data Catalog Listing

means to find the times when the spacecraft is not transmitting.

The integrate and dump samples themselves can be used to calculate the radiometric power, however, the presence of a DC bias in the sampled data being filtered makes this somewhat more complex. An estimate of the DC offset of the sampling process is subtracted, however, the estimate is of limited precision, so there is a remaining offset that must be taken into account.

Consider the term being summed in (3), above,

$$x_i^2 = (\tilde{x}_i + b)^2$$

where  $\tilde{x}_i$  is the true value, and  $b$  is the remaining bias. Expanding the squared term, we get:

$$\tilde{x}^2 + 2\tilde{x}b + b^2$$

However,  $\tilde{x}$  is assumed to be a zero mean random process, so when summed, the  $2\tilde{x}b$  term falls out, leaving the true variance estimate and a constant equal to the square of the dc offset. The actual DC offset can be measured by integrating the A/D output with the receiver connected to a known noise source. The bias term is then the difference between the measured offset and the estimated offset used in calculating the integrate and dump

dataset.

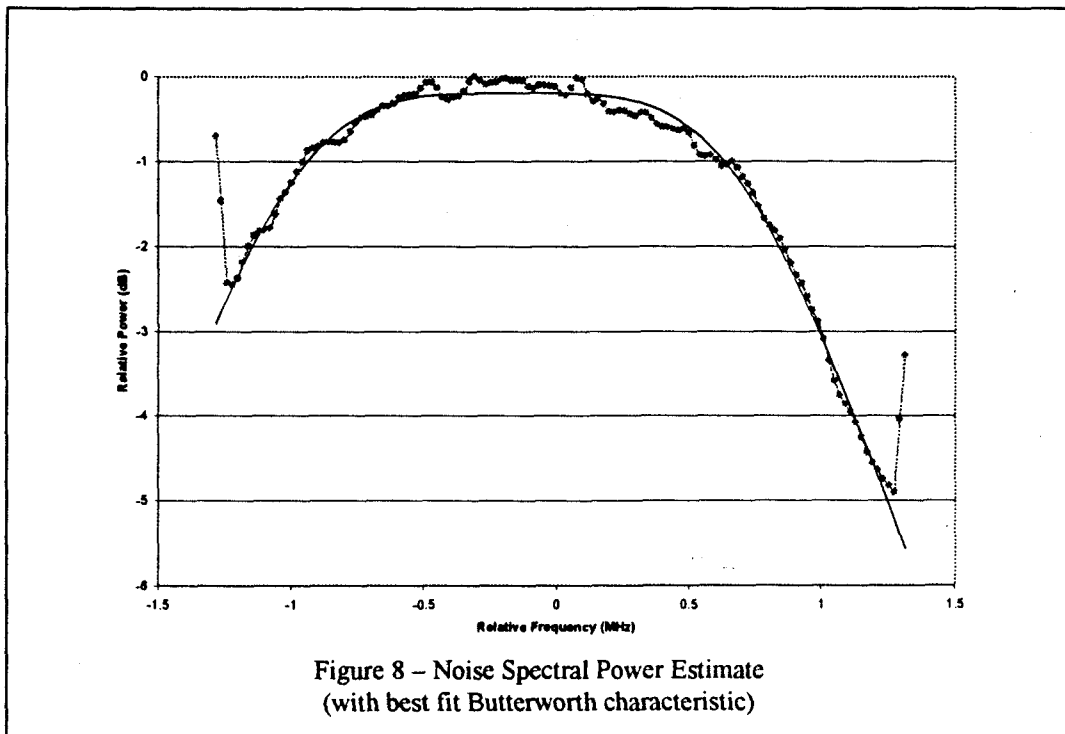
#### Refinement of noise power measurement

When calculating the system gain, in an absolute sense, changes in the noise bandwidth  $B$ , in equation (1), above, cause proportional changes in the calculated gain. This noise bandwidth is set by an analog filter in the receiver chassis. The temperature of this filter is relatively constant, however it does change, and its aging behavior is unknown.

There are also potential interfering low level signals which have been observed at random intervals, although always at the same frequency. These interfering signals don't make a significant difference in the primary CGS role of digitizing and analyzing the spacecraft transmitter signals, but they do contribute to low level radiometric measurements.

We can improve our estimate of the noise bandwidth and excise the interfering signals by applying a digital filtering approach to artificially restrict the measurement bandwidth. The sample rate of the CGS is very accurately controlled, so a computational filter which depends on the sample rate will also have a stable bandwidth.

The approach taken is to form an estimate of the power in a relatively small number of equally



spaced frequency bins. We use the method recommended by Yuen<sup>4</sup>, which uses a windowed Discrete Fourier Transform of a series of zero padded autocorrelations. The actual implementation doesn't compute the explicit autocorrelation, but uses the transform of the autocorrelation instead.

With the use of 128 bins, each nominally 20 kHz wide, we can avoid using those frequencies which have interfering signals, or system noise near the folding frequencies. The power in the selected bins is summed, creating a filter with known noise bandwidth. Figure 8 illustrates the results of this process with a Butterworth bandpass characteristic superimposed.

#### Observation Schedule

The orbit of the spacecraft is such that it repeats every 4 days with a high degree of accuracy (nominally 1 km). The times and look angles for the beam crossings repeat on the same 4 day cycle. There are 2 days on which both inner and outer beams cross the CGS, 1 day when only the outer beam crosses, and 1 day when the spacecraft doesn't get high enough in the sky so that any beams cross. Table 1 is a canonical capture schedule for the CGS, based upon the orbit as of October 1999. All times are in UTC, and look angles are (azimuth, elevation) relative to true north and local horizontal. The 0100Z captures are referred to as evening captures because they occur at about 7PM local, and the 1200Z captures are referred to as morning captures because they occur at about 6AM local.

#### Scheduling Mechanics

Every day, at 18Z (noon local), an ephemeris file that has predicted Earth Centered Inertial (ECI) x,y,z coordinates of the spacecraft at 1 minute intervals for the next 5 days is FTP'd to the CGS. At 22Z, a series of programs is run which use these positions to determine when the spacecraft is above the nominal horizon, relative to the CGS. During the above horizon periods, cubical interpolation to calculate look angles from the CGS at successively finer intervals (to 0.1 second) to identify the times and look angles of the beam crossings, assuming the nominal 40 and 46 degree nadir angles from the spacecraft. From these data, scheduling files are created which control the digitizing and pedestal processes on a daily basis. At 23Z, the schedule for the next 24 hours is put in place, and the captures occur as scheduled. Overriding the default schedule is possible by editing the schedule files to accommodate unique situations, and, as well, the software is being enhanced to allow a more convenient interface for this function.

### 5. SAMPLE SPACECRAFT SIGNAL MEASUREMENTS

We present some typical capture data from a capture at 01:38:26Z on 26 October 1999. A 20 second capture window around the predicted time that the outer beam would cross the CGS was 01:38:36Z was processed. UTC is 6 hours ahead of local time (MDT) at the CGS, so this capture actually occurred about 7:30 PM in the evening on 25 October 1999.

Table 1 - Canonical Capture Schedule

	<i>Outer Beam Approaching</i>	<i>Inner Beam Approaching</i>	<i>Inner Beam Receding</i>	<i>Outer Beam Receding</i>
Day 1: (10 Seconds)	01:38:36 (350.9,36.6) 12:53:50 (191.6,36.2)	01:39:17 (343.4,44.3) 12:54:30 (199.1,44.0)	01:42:17 (227.7,43.9) 12:57:31 (317.99,44.2)	01:42:40 (220.1,36.2) 12:58:11 (325.0,36.5)
Day2: (10 Seconds)	01:13:34 (25.0,36.6) 12:28:47 (151.3,36.2)	01:14:11 (28.4,44.3) 12:29:26 (147.77,44.0)	01:17:29 (176.3,43.9) 12:32:41 (3.07,44.3)	01:17:54 (179.9,36.1) 12:33:20 (359.1,36.5)
Day 3: (20 Seconds)	00:49:37 (69.5,36.5) 12:05:11 (102.4,36.3)			00:51:49 (129.5,36.2) 12:07:24 (42.0,36.5)
Day 4:				

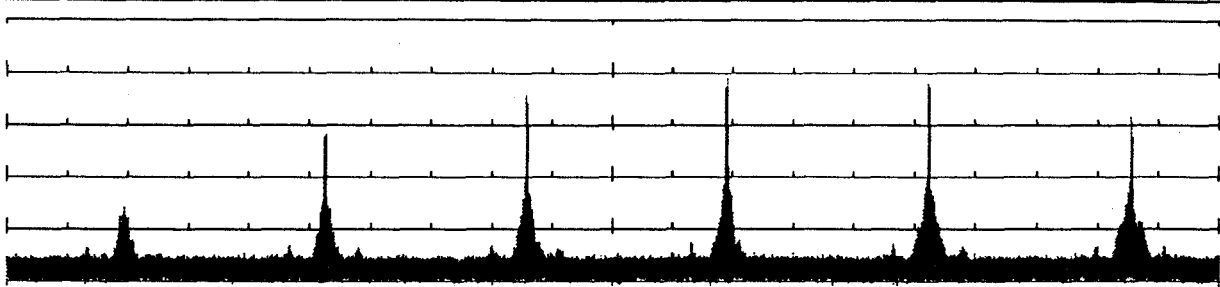


Figure 9a – 20 second capture of outer beam crossing  
V: 10 dB/division, H: minor ticks at 1 second intervals

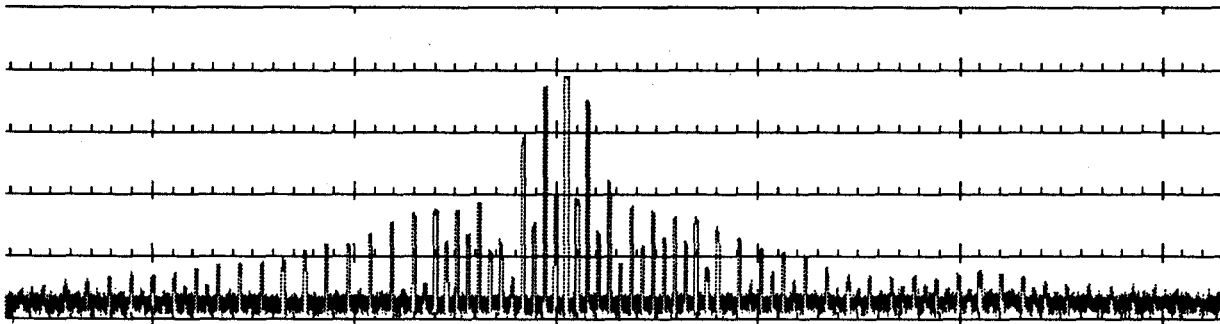


Figure 9b - Outer beam crossing  
V: 10 dB/division, H: 0.1 Second/major division

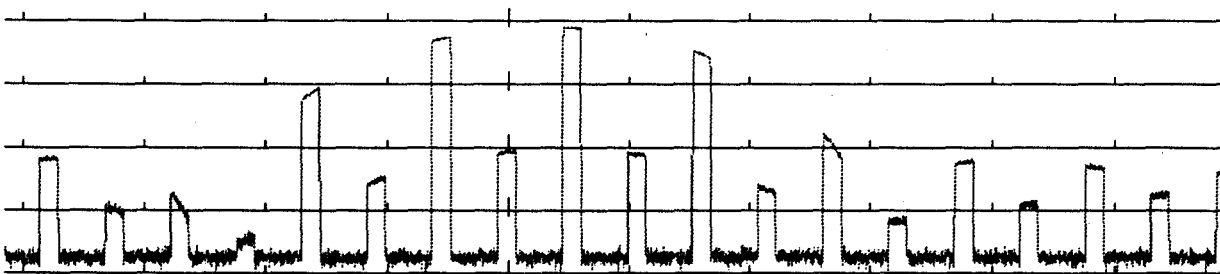


Figure 9c – Outer Beam Crossing, main lobe detail  
V: 10 dB/division, H: 10 mSec/minor division

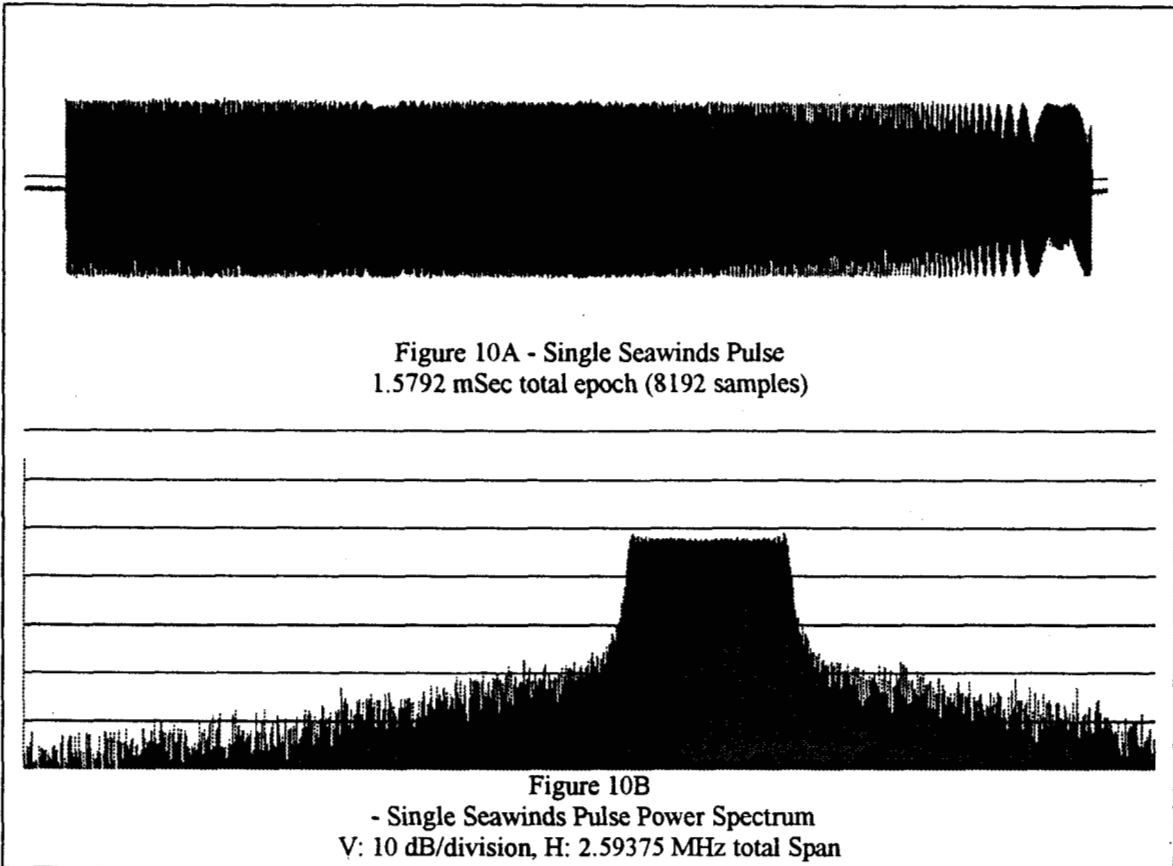


Figure 9 presents a series of log scaled plot of the integrate and dump dataset. This is the equivalent of the "log video" output from an analog receiver. The first plot (Fig. 9A shows the data for an entire 20 second capture as the outer beam crosses the CGS. The 3.3 second period of the spacecraft antenna rotation is visible, as multiple passes corresponding to successive "elevation cuts" across the pattern. Some small sidelobe about 30 dB down, and 60 degrees off boresight are also visible.

In the next two plots, Figures 9B and 9C, the central area is expanded showing more detail of the pulse envelopes. The detailed envelope of the spacecraft antenna is visible, as well as the power received from the side lobes of the inner beam. By fitting the measured spacecraft antenna pattern to the received data, it is possible to estimate where the "peak" of the pattern would be, and hence the absolute azimuth/yaw orientation of the spacecraft antenna at that time.

Figure 10 presents time and frequency domain plots of a single Seawinds radar pulse. In Figure 10A, the time domain plot, the chirped nature of the pulse is quite evident, with a signal to noise

ratio of about 30 dB. Seawinds pulses are down chirps with a chirp bandwidth of 375 kHz, and this pulse is centered at about 250 kHz from the nominal center frequency.

Figure 10B is the power spectrum of the same pulse. The characteristic flat topped appearance of a chirped pulse is evident. The particular frequency folding from undersampling results in the frequency scale being inverted, so that high input frequencies appear at the left end of the plot.

## 6. CONCLUSIONS

The Seawinds CGS is a high performance self calibrating autonomous measurement receiver which provides accurate measurements of the timing and amplitude of pulses from the Seawinds Ku-band Scatterometer. The precisely timed data collected by the CGS referenced to a high quality time standard allows determination of spacecraft timing, clock, and attitude offsets with an independent source of data. This was particularly valuable in the first weeks after instrument turn on when the spacecraft attitude was not yet stabilized<sup>6</sup>.

Future work is planned with the CGS to further characterize various aspects of the system, such as long term gain stability and refined path and radome loss estimates. Further enhancements to CGS operations will result from the practical experience gained with actual spacecraft data and evolving user requirements.

The CGS will also receive and process signals from the second Seawinds instrument scheduled to be launched in late 2000 on ADEOS II. The stable and repeatable measurement capability provided by the CGS, will provide a consistent reference to compare the performance of the two spaceborne instruments.

#### ACKNOWLEDGEMENTS

The research described in this paper was carried out by the Jet Propulsion Laboratory, California Institute of Technology, under a contract with the National Aeronautics and Space Administration.

The Seawinds CGS wouldn't be a reality without the hard work of Scot Stride, Quintin Ng, and Dominic Wu. the reviews, advice, and assistance of D. Long and his students at BYU, and the support of everyone in the SeaWinds project at JPL.

#### REFERENCES

- [1] D. G. Long and M. W. Spencer, "Performance Analysis for the SeaWinds Scatterometer," *Proceedings of the International Geoscience and Remote Sensing Symposium*, Lincoln, Nebraska, 27-31 May, pp. 1463-1465, 1996.
- [2] B. L. Seidel and C. T. Stelzreid, "A Radiometric Method for Measuring the Insertion Loss of Radome Materials", *IEEE Trans. MTT* MTT-46, 625, 1968.
- [3] C. T. Stelzreid and M. S. Reid, "Precision Power Measurement of Spacecraft CW Signal Level with Microwave Noise Standards", *IEEE Trans. Instrumentation and Measurement* IM-15, 318, 1966.
- [4] C. K. Yuen, "A Comparison of Five Methods for Computing the Power Spectrum of a Random Process using Data Segmentation", *IEEE Proceedings* 65, 984-986, June 1977.
- [5] Clague, F.R., *NIST model PM2 power measurement system for 1mW at 1GHz*, NISTIR 5016, Dec 1993, NIST Boulder CO

- [6] D.G. Long, P. Yoho, A. Anderson, J. Adams, J. Lux, T. Cheng, "Results from the SeaWinds Calibration Ground Station", *SeaWinds Cal/Val Work Shop Meeting*, Pasadena, CA, 2-5 Nov, 1999.



**Jon T. Adams** is a senior member of the technical staff at Caltech's Jet Propulsion Lab in addition to being manager of the Flight Digital Radio Subsystems group, which develops and supports both earth-orbiting radar and deep space telecom solutions.



**James Lux** is in the Flight Digital Radio Subsystems group at JPL. Calibration of scatterometers is only one of Jim's diverse interests, which range from man-made tornadoes to solar eclipses to high performance digital radio links.